Food Chemistry: Molecular Sciences 1 (2020) 100004

Contents lists available at ScienceDirect

Food Chemistry: Molecular Sciences

journal homepage: www.elsevier.com/locate/fochms

Transcriptome and metabolome analyses reveal the regulation of peel coloration in green, red Chinese prickly ash (*Zanthoxylum* L.)

Tao Zheng, Qun Zhang, Ke-xing Su, Shu-ming Liu *

College of Science, Northwest A & F University, Yangling, Shaanxi 712100, China

ARTICLE INFO

Keywords:
Chinese prickly ash (*Zanthoxylum piasezkii* Maxim., *Zanthoxylum armatum* DC., *Zanthoxylum bungeanum* Maxim.)
Anthocyanins
Flavonoid
Transcriptome
Metabolome
Peel coloration

ABSTRACT

Peel colour is an important external economic characteristic of Chinese prickly ash cultivars (*Zanthoxylum bungeanum* Maxim.). To gain insight into their coloration mechanisms, we performed an integrated analysis of green and red peels using combined metabolomic and transcriptomic analyses. Pelargonin-O-hexoside-O-rhamnoside-O-hexoside, pelargonidin 3,5-diglucoside, peonidin O-hexoside, cyanidin O-syringic acid and peonidin 3-O-glucoside were found to be the key anthocyanins. Transcriptome data indicated that the anthocyanidin synthase genes and UDP-glucose flavonoid 3-O-glucosytransferase genes were significantly increased to promote the redness of the peels. In addition, we discussed the role of R_2R_3-MYB transcription factors in coloration, of which the c80935 and c226097 genes may be the key regulatory factors for anthocyanin biosynthesis. Generally, this is the first study to identify and reveal the main anthocyanins in Chinese prickly ash peels during different developmental periods. The results of this research lay the foundation for understanding the regulation of coloration in Chinese prickly ash peels.

1. Introduction

Chinese prickly ash (*Zanthoxylum bungeanum* Maxim.), of the Zanthoxylum genus belonging to the family Rutaceae, is a deciduous shrub native to East Asian countries (Liu et al., 2019; Yu et al., 2020). In China, Chinese prickly ash has a long history of nearly three thousand years of cultivation. Owing to its high nutritional value and numerous pharmacological effects, Chinese prickly ash has become an economically important fruit tree, and its peels are commonly utilized as a food additive, for flavouring, and as a Chinese medicine due to their fragrance and distinctive taste (Artaria et al., 2011; Sun et al., 2019; Wu et al., 2018). Its planting area is more than 1.5 million hm^2, and the annual output of dried peppers is nearly 12 kilotons, corresponding to a value of ca. 7 billion yuan, which are the largest in the world (Chen, Wang et al., 2019).

The fruit peel is the boundary of the fruit, protecting it from damage by the external environment and maintaining fruit integrity. Secondary metabolites in the peel, such as pigments, tannins and aroma compounds, affect fruit appearance, quality and storage. The colour and flavour quality are important commodity traits of the fruit (Li et al., 2013; Zhang et al., 2020); therefore, it is of great industrial significance to study the accumulation and regulation of anthocyanin substances in Chinese prickly ash peels.

Anthocyanin derivatives of pelargonidin, cyanidin, delphinidin, peonidin, petudinin and malvidinare with biological activities, antioxidant activity, antiaging activity and the ability to reduce the risk of cancers and diabetes (Ellinger et al., 2012; Wang, Cui et al., 2017; Zhang et al., 2020), commonly exist in coloured fruit in the form of glycosylation, whereas derivatives of cyanidin and pelargonidin are the main pigments in bright-red-coloured fruits (Jaakola, 2013). In addition, they also play important basic physiological functions in plants (Gharibi et al., 2019; Hodaei et al., 2018; Winkel-Shirley, 2002; Yang et al., 2008), including UV protection (Poulose et al., 2012), pigmentation of flowers and fruits to attract pollinators and seed transmission, and responses to biological and environmental stress (Hodaei et al., 2018). Studies of peel coloration mechanisms have indicated that anthocyanin metabolism is catalysed by structural biosynthetic genes and transcription factors (Milbury, 2015; Rothenberg et al., 2019). Structural biosynthetic genes, including phenylalanine ammonia-lyase (PAL), 4-coumarate:coenzyme A ligase (4CL), chalcone synthase (CHS), chalcone isomerase (CHI), flavanone 3-hydroxylase (F3H), flavanone 3′-hydroxylase (F3′H), flavonoid 3′5′-hydroxylase (F3′5′H), dihydroflavonol 4-reductase (DFR), anthocyanidin synthase (ANS) and UDP-glucose: flavonoid 3-O-glucosyltransferase (UFGT), lead to the accumulation of different types and quantities of anthocyanins in plant tissues, resulting in different

* Corresponding author.
E-mail address: liusm@nwsuaf.edu.cn (S.-m. Liu).

https://doi.org/10.1016/j.fochms.2020.100004
Received 11 July 2020; Revised 14 October 2020; Accepted 17 October 2020
Available online 22 October 2020

chromasines (Zhuang et al., 2019; Saito et al., 2013). The synthesis of anthocyanins is also regulated by various transcription factors, such as MYB transcription factors (MYB TFs), basic helix-loop-helix (bHLH) and WD40-like proteins (Liu et al., 2016; Ohno et al., 2011; Petroni & Tonelli, 2011; Sepulveda et al., 2010; Shoeva et al., 2014). Recently, HD-Zip, NAC and H_2C_2 TFs have also been shown to regulate the genes involved in anthocyanin biosynthesis in blood-flesh peaches and jujube peel (Zhang et al., 2020; Zhou et al., 2015).

Moreover, anthocyanin derivatives affect the colour and taste of peels, and their antioxidant and nutritional abilities impart health properties and reduce the risk of cardiovascular disease and mortality (Fragoso et al., 2018; Kruger et al., 2014). Therefore, the genetic regulation mechanism of identifying and analysing anthocyanin metabolites has become an important subject in the study of plant secondary metabolism (Liu et al., 2018). However, insights into the regulation of the anthocyanin biosynthesis pathway in Chinese prickly ash remain unclear. Understanding the genetic basis of peel coloration traits will help growers and consumers determine the ripeness and quality of the fruit, which is conducive to access more attractive and healthier fruits (Pojer et al., 2013).

Recently, advances in high-throughput functional transcriptomics and metabolomics methods have been applied to research in genes regulating fruit peel coloration (Chen, Zhang et al., 2019; Cho et al., 2016; Gao et al., 2020; Wang, Du et al., 2017). In this study, we used a combination of transcriptome and metabolome analysis to explore the regulatory network of anthocyanin biosynthesis in the green peel and red peel of three Chinese prickly ashes (*Zanthoxylum piasezkii* Maxim; *Zanthoxylum armatum* DC; *Zanthoxylum bungeanum* Maxim.). We were interested in the differential expression of anthocyanin metabolites and their key regulatory genes and mapped the connected network based on the analysis of metabolites and transcripts to highlight the regulatory genes related to anthocyanin metabolites. Our research provides new insight into the molecular mechanisms of the biosynthesis and regulation of anthocyanins during accumulation in the pigmentation of Chinese prickly ash cultivars.

2. Materials and methods

2.1. Peel materials

The three Chinese prickly ash cultivars were cultivated in a common garden in Yangling City (34°15′N, 108°03′E), Shaanxi Province, China. The soil type is lou soil. Each peel was sampled with more than 3 consistent growth material samples, of no less than 3 g with three replicates, uniform in shape, size and colour, with no signs of mechanical damage or disease, loaded in a 10 ml centrifuge tube, and quickly transported to the laboratory (Chen, Wang et al., 2019; Zhang et al., 2016). The green peels were collected on 15 May 2019, and the full-red peels were collected on 25 August 2019, soon after ripening. All the peels (approximately 2 mm) were carefully excised with a razor blade, collected, frozen in liquid nitrogen for 2 min, and kept at −80 ℃ for further use. Peels at different developmental stages were extracted from the three cultivars, called “green peels” young fruit (CY, ZY, HY) and “red peels” mature fruit (CM, ZM, HM) (Fig. 1). Finally, six samples (CY, ZY, HY, CM, ZM, HM) of three biological replicates (18 samples in total) were used for further analysis.

2.2. Metabolite extraction

The sample extraction analysis, metabolite identification and quantification were conducted at MetWare Biotechnology Co., Ltd. (www.metware.cn; Wuhan, China) following their standard procedures (Lu et al., 2020; Yang et al., 2008; Zhang et al., 2017). The analysis of metabolite data was performed using Analyst 1.6.1 software (AB SCIEX, Ontario, Canada). Multiple statistical analysis methods, including principal component analysis (PCA) or orthogonal partial least squares-discriminant analysis (OPLS-DA), were used to screen difference variables to determine interspecies and intraspecies differential metabolites based on PCA model results and OPLS-DA model result variable importance in projection (VIP). The screening of significantly different metabolites was followed by variable importance in projection (VIP) ≥ 1 and fold change ≥2 or ≤0.5 (Baldi et al., 2018; Jin et al., 2019).

2.3. RNA-seq and annotation

The experimental process of transcription group sequencing included RNA extraction, RNA detection, and the construction of cDNA libraries, as performed previously (Chai et al., 2017; Lu et al., 2020). The libraries were sequenced on an Illumina HiSeq platform, and 150 bp paired-end reads were generated. The unigene sequences were compared to the KEGG (Kyoto Encyclopedia of Genes and Genomes), NR (NCBI nonredundant protein sequences), Swiss-Prot (a manually annotated and reviewed protein sequence database), GO (Gene Ontology), COG/KOG (Clusters of Orthologous Groups of proteins/euKaryotic Orthologue Groups) and Trembl databases using BLAST V2.7.1 software (Chai et al., 2017). After predicting the amino acid sequence of the unigenes, HMMER software was used to obtain annotation information for the unigenes compared to the Pfam database.

2.4. Transcriptome data analysis

The amount of gene expression was expressed in the words FPKM (Fragments Per Kilo bases per Million Reads) using featureCounts v1.5.0-p3 (Liao et al., 2014), which represented the number of fragments per thousand base length of a gene per million fragments (Dong et al., 2019; Zhang et al., 2015). It is generally believed that a value greater than 1 indicates that the gene had been expressed, while a value of less than 5 indicates that the expression was lower. Differentially expressed genes (DEGs) were recruited by log2 (fold change) ≥ 1 and corrected P ≤ 0.005 (Li et al., 2020; Polturak et al., 2018). All DEGs were analysed by gene ontology (GO) enrichment using GO seq (1.10.0) and Kyoto Encyclopedia of Genes and Genomes (KEGG) enrichment using KOBAS software.

2.5. Real-Time quantitative PCR (RT-qPCR) validation

We chose the anthocyanidin biosynthesis genes and MYB TFs in the RNA-seq data for RT-qPCR validation. Specific quantitative primers were designed using Primer 5.0 software based on the *Zanthoxylum* L genome reference sequence (Table S1). RT-qPCR was performed with a Step One PULS Real-Time Detection System (ABI, Foster, CA, USA) using 2X SG Fast qPCR Master Mix (High Rox, B639273, BBI, ABI). The amplification system in a total volume of 20 μL consisted of 10 μL of SybrGreen qPCR Master Mix, 0.4 μL of F primer, 0.4 μL of R primer, 7.2 μL of ddH_2O, and 2 μL of cDNA. All relative quantitative analysis of validation genes was performed by the $2^{-\Delta\Delta\ Ct}$ method with reference genes UBQ. The expression levels of anthocyanin biosynthetic genes and regulatory genes, including the ANS genes, UFGT genes and MYB TFs, were determined simultaneously with three technical replicates.

3. Results

3.1. Metabolite assay in three Chinese prickly ash cultivars

There were significant differences in the flavonoid metabolites in green peels and red peels. A total of 194,176,193 metabolites were identified from CY_vs_CM, ZY_vs_ZM, and HY_vs_HM samples, each with three biological replicates. We observed that all biological repli-

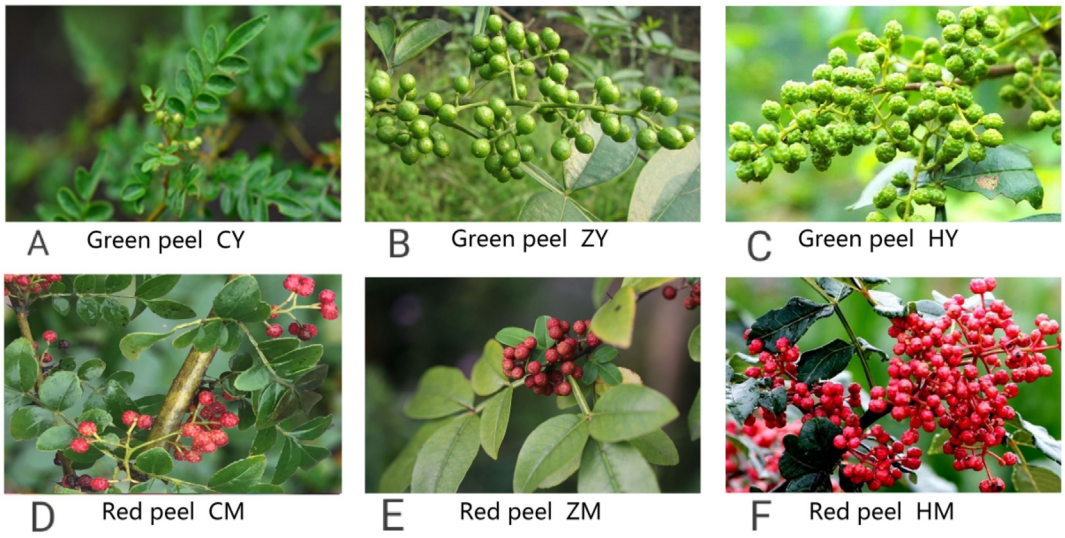

Fig. 1. The phenotype of three Chinese prickly ash cultivars, green peel and red peel, at young and mature stages. A: "CY" *Zanthoxylum piasezkii* Maxim green peel; B: "ZY" *Zanthoxylum armatum* DC green peel; C: "HY" *Zanthoxylum bungeanum* Maxim green peel; D: "CM" *Zanthoxylum piasezkii* Maxim red peel; E: "ZM" *Zanthoxylum armatum* DC red peel; F: "HM" *Zanthoxylum bungeanum* Maxim red peel. (For interpretation of the references to colour in this figure legend, the reader is referred to the web version of this article.)

cas were grouped together, indicating a high reliability of the generated metabolome data. Setting VIP ≥ 1.0 together with fold change ≥2 or ≤0.5 as thresholds for significant differences, the 4 categories and 15 kinds of metabolites were significantly different in CY_vs_CM (Table 1); the 5 categories and 18 kinds of metabolites were significantly different in ZY_vs_ZM (Table S2); and the 5 categories and 19 kinds of metabolites were significantly different in HY_vs_HM (Table S3).

3.2. Analysis of anthocyanins, flavonoids and flavonols in Chinese prickly ash cultivars

Anthocyanins are the most important flavonoid colorants in plants. A total of 10 anthocyanins were found in the three varieties, including pelargonin-O-hexoside-O-rhamnoside-O-hexoside (Pel-rha), pelargonidin 3,5-diglucoside (Pel-3,5-diglu), cyanidin O-syringic acid (Cya-O-sya), peonidin O-hexoside (Peo-O-hex), peonidin 3-O-glucoside (Peo-3-O-glu), cyanidin 3-O-glucoside (Cya-3-O-glu), cyanidin 3-O-galactoside (Cya-3-O-gal), peonidin (Pn), malvidin 3-O-glucoside (Mal-3-O-glu), and malvidin 3-O-galactoside (Mal-3-o-glu); yet pel-rha, pel-3,5-diglu, cya-O-sya, peo-O-hex, and peo-3-O-glu might be the main anthocyanins. In the mature stage, the accumulation of anthocyanin glucosin pigment caused the peel to appear red. Pel-rha and Pel-3,5-diglu in CM increased by 7.73E + 02- and 1.11E + 03-fold compared with CY, which resulted in CM being brick red (Fig. 1D); peo-O-hex, cya-O-sya, and peo-3-O-glu increased by 1.40E + 01-, 1.17E + 01- and 1.03E + 01-fold in ZM, resulting in being dark red (Fig. 1E); and peo-O-hex and peo-3-O-glu increased by 5.36E + 05-, 4.89E + 05-fold in HM, leading to being bright red (Fig. 1F). The increase in anthocyanin-glucosin pigment in HM and

Table 1
Differentially accumulated flavonoid compounds in the green and red peels of *Zanthoxylum piasezkii* Maxim.

Index	Compounds	CY	CM	VIP	Fold_Change
Flavanols	(−)-Epigallocatechin	1.10E+06	1.01E+07	1.40E+00	9.17E+00
	(+)-Gallocatechin	4.93E+05	6.43E+06	1.51E+00	1.30E+01
	Kampferol 3-O-(6″-galloyl)-β-D-glucopyranoside	6.63E+03	1.52E+04	1.11E+00	2.28E+00
	Kaempferin	9.00E+00	1.36E+04	2.55E+00	1.51E+03
	Quercetin-O-rhamnoside-O-pentoside	7.82E+04	9.00E+00	2.83E+00	1.15E−04
	Kaempferol glucuronic acid	1.25E+05	9.00E+00	2.88E+00	7.19E−05
Flavonoid	Myricetin-3,7-O-dirhamnoside	2.13E+05	1.84E+06	1.38E+00	8.64E+00
	Eriodictyol-7-O-glucoside	1.01E+06	4.02E+06	1.11E+00	3.97E+00
	Apigenin-7,4′-dimethylether	5.79E+03	2.15E+04	1.08E+00	3.71E+00
	Apigenin-7-O-(6-O-malonyl glucoside)	3.05E+04	9.00E+00	2.69E+00	2.95E−04
	Chrysoeriol 6-C-hexoside 8-C-hexoside-O-hexoside	5.57E+04	9.00E+00	2.78E+00	1.62E−04
Anthocyanins	Pelargonin-O-hexoside-O-rhamnoside-O-hexoside	9.00E+00	6.96E+03	2.42E+00	7.73E+02
	Pelargonidin 3,5-diglucoside	9.00E+00	1.00E+04	2.50E+00	1.11E+03
Dihydroflavone	Eriodictiol-O-rhamnoside-O-pentoside-O-glucuronate	1.17E+05	1.40E+06	1.48E+00	1.19E+01
	Hesperetin	1.81E+05	6.13E + 05	1.04E+00	3.38E+00

Note: Metabolite fold changes, value >1.0 represents increase; value <1.0 represents decrease. Differentially accumulated flavonoid compounds were identified by threshold VIP (variable importance in projection) ≥ 1 and fold change ≥ 2 (upregulation) or ≤ 0.5 (downregulation).

the peel colour were better than that of CM and ZM, which explained that HM was the main plant variety.

Among the monomeric flavonoids, (−)-epigallocatechin, (+)-gallocatechin, kampferol 3-O-(6″-galloyl)-β-D-glucopyranoside, and kaempferin showed markedly higher contents in the CM, of which kaempferin was 1.51E + 03-fold higher than CY; quercetin-O-rhamno side-O-pentoside and kaempferol glucuronic acid in CY decreased by 1.15E-04- and 7.19E-05-fold, respectively (Table 1). Compared with ZY, the contents of kaemPferol-3,7-O-α-L-rhamnoside, quercetin glucuronic acid, methylquercetin rhamnoside, and quercetin in ZM was significantly increased, and the highest increase was kaempferol-3,7-O-α-L-rhamnoside, which increased by 9.16E-02-fold, whereas the content of (-)-epigallocatechin and catechin gallate decreased by 1.32E-04- and 5.64E-02-fold, respectively (Table S2). In HM samples, vitexin, isovitexin, kaempferol3-O-α-L-rhamnoside-(X), isorhamnetin, and di-O-methylquercetin demonstrated significantly higher contents; di-O-methylquercetin was 7.74E + 00-fold of HY content; and (-)-epicatechingallate and gallocatechin-gallocatechin in HY decreased 1.51E-03- and 2.09E-04-fold, respectively (Table S3).

For the flavones, the contents of myricetin-3,7-O-dirhamnoside, eriodictyol-7-O-glucoside, and apigenin-7,4′-dimethylether in CM were 8.64E + 00-, 3.97E + 00-, and 3.71E + 00-fold higher than those in CY, while the contents of apigenin-7-O- (6-O-malonyl glucoside) and chrysoeriol 6-C-hexoside 8-C-hexoside-O-hexoside in CY significantly decreased 2.95E-04- and 1.62E-04-fold (Table 1). Compared to ZY, apigenin 5-O-glucoside and limocitrin3,7-diglucoside contents revealed marked increases of 9.64E + 03- and 3.73E + 02-fold in ZM, while the content of acacetin-O-glucuronic acid and chrysoeriol 7-O-hexoside in ZY demonstrated significant decreases of 7.95E-04- and 1.58E-05-fold (Table S2). In HM, the naringenin-7-O-triglycoside, 7,8-dihydroxy-5,6,4′-teteamethoxyflavone, and acacetin-O-glucuronic acid contents were significantly higher, with 6.33E + 02-, 5.34E + 04-, and 1.61E + 02-fold increases; however, limocitrin-O-pentoside showed a decrease of 1.34E-01-fold (Table S3).

3.3. Transcriptome analysis of three Chinese prickly ash cultivars

cDNA libraries for the young and mature fruit periods of three *Zanthoxylum* L cultivar samples were constructed. Eighteen samples were sequenced using the Illumina NovaSeq 6000 sequencing platform to obtain 133.61 Gb clean data, each with 6 Gb, and the Q30 base percentage was 92% and above. Using Trinity software to assemble raw read transcripts, 406,061 transcripts with an average length of 398 bp, the longest cluster sequence of the Corset hierarchy, 281,472 unigenes, N50 515 bp, and a total base of 131441020 bp were obtained. Comparing the assembled Unigenes with KEGG, NR, SwissProt, Trembl, KOG, GO and Pfam databases, the final annotation results are 133,562 (KEGG: 47.45%), 186,859 (NR: 66.39%), 122,508 (SwissProt: 43.52), 185,801 (Tbl) 101,994 (KOG: 36.24%), 145,178 (GO: 51.58%) and 103,952 (Pfam: 36.93%).

Venn diagrams of samples CY_vs_CM, ZY_vs_ZM, and HY_vs_HM showed that the three groups produced 861 common genes (Fig. S1A). There were 35265, 6540, and 20,409 DEGs of the three cultivars, of which 16773, 3199, and 10,809 genes were upregulated and 18492, 3341, and 9600 genes were downregulated (Fig. S1B). Based on the annotation results of the Swiss-Prot and Trembl databases, GO annotations were made using BLAST V2.7.1, which was divided into three main categories: biological process, cell component and molecular functional class. The GO database reviewed 145,178 (51.58%) of 281,472 unigenes, including 28 biological processes, 18 cellular components and 14 molecular functional classes (Fig. S2). The overall annotation results showed that the most GO annotations obtained by “biological processes” with two main components, cellular processes (GO:0009987, 60.92%) and metabolic processes (GO:0008152, 53.05%), followed by biomodulation (GO:0065007, 28.50%), reaction to stimulation (GO:0050896, 28.43%) and bioprocess regulation (GO:0050789, 25.95%); in “cell composition”, the cell (GO:0005623, 72.82%) and the cell part (GO:0044464, 72.69%) were the two main parts, followed by the organelle (GO:0042226, 56.29%) and membranes (GO:0016020, 37.19%), with combination (GO:0005488, 61.34%) and catalytic activity (GO:0003824, 48.17%) the two main components.

KEGG analysis revealed phenylpropanoid biosynthesis, biosynthesis of secondary metabolites, plant hormone signal transduction, and metabolic pathways as the significantly changed pathways in CY_vs_CM and ZY_vs_ZM. Starch and sucrose metabolism, phenylpropanoid biosynthesis, biosynthesis of secondary metabolites, and metabolic pathways were significantly changed in HY_vs_HM (Table 2).

3.4. Modulation of the anthocyanidin biosynthesis pathway of three Chinese prickly ash cultivars

In the peels from green to red, most secondary metabolic pathways are strengthened in the “red skin” fruit by increased gene expression, while the structural genes of phenylpropic acid, flavonoids and anthocyanin biosynthesis, including CHS, CHI, F3H, F3’H, FR/DFR, ANS and UFGT, were largely increased. High fold upregulation enhanced the flux in the flavonoid and anthocyanidin biosynthetic pathways (Fig. 2). The structural genes of CHS (c182455, c117369, c141881) showed 2.78-fold, 2.44-fold and 1.44-fold increments, the CHI genes (c.148658, c123303, c146046) demonstrated 1.12-fold, 1.34-fold, and 1.21-fold upregulation, and the F3H genes (c96315, c98861, c131310) underwent 2.07-fold, 2.76-fold, and 1.25-fold upregulation, respectively. In the *Zanthoxylum piasezkii* Maxim. cultivar, the F3’H gene (c158354) was downregulated to prevent dihydrokaempferol from producing dihydroquercetin, and the FR/DFR genes (c158341, c97481) were upregulated to promote the accumulation of lecupelargonidin in the mature period; together with two FLS genes (c168971, c157503) that catalysed the transformation of dihydrokaempferol to kaempferol, and two FLS genes (c128993, c158354) that downregulate the conversion of kaempferol to quercetin, which illustrated the accumulation of kampferol 3-O-(6″-gal loyl)-β-D-glucopyranoside, kaempferin, the reduction of quercetin-O-rhamnoside-O-pentoside. Due to the reduction in two LAR genes (c196329, c24474), LAR genes activated and promoted leucodelphindin conversion to (+)-gallocatechin and delphindin conversion to (−)-epigallocatechin. Pelargonin was generated from lecupelargonidin catalysed by the ANS gene (c158341), and then pelargonin-3-O-glucoside (Pel-3-O-glu) was produced from pelargonin catalysed by the UFGT gene (c144425). UDP-glycosyltransferase 75C1 catalysed pel-3-O-glu to pel-rha and pel-3,5-diglu, showing the high measured accumulation of anthocyanidin in CM peel. In *Zanthoxylum armatum* DC. cultivars, the FLS genes not only catalysed the conversion of kaempferol to quercetin but also naringenin to apigenin, which explained the accumulation of hesperetin-7-O-glucoside and apigenin 5-O-glucoside, while in the *Zanthoxylum bungeanum* Maxim cultivar, the FLS genes catalysed naringenin to produce eriodictiol, indicating a large increase in eriodictiol-O-rhamnoside-O-pentoside-O-glucuro nate. In *Zanthoxylum armatum* DC and *Zanthoxylum bungeanum* Maxim varieties, F3’H genes (c158354, c128993, c63210) were upregulated to promote dihydrokaempferol to produce dihydroquercetin, and under the catalysis of DFR, leucocyanidin was produced. The ANS genes (c158341, c99788, c97481, c125833) accelerated the accumulation of cyanidin from leucocyanidin. All UFGT genes (c164027, c130493) were increased, to form cya-3-O-glu, peo-O-hex, cya-O-sya and peo-3-O-glu in the red peels produced by cyanidin-3-O-glucoside, explaining the high accumulation of peo-O-hex, cya-O-sya, peo-3-O-glu in ZM and peo-O-hex, peo-3-O-glu in HM.

Table 2
Significantly enriched KEGG pathways between "green Peel" and "red Peel" from three Chinese prickly ash cultivars.

NO.	Pathway	DEGs with pathway annotation	All genes with pathway annotation	P-value	Corrected P-value	Pathway ID
CY_vs_CM	Plant hormone signal transduction	742	3317	0	0	ko04075
	Phenylpropanoid biosynthesis	509	1803	5.08186E−11	7.21624E−09	ko00940
	Metabolic pathways	5355	26,138	0	0	ko01100
	Biosynthesis of secondary metabolites	3042	13,445	3.89981E−11	5.53774E−09	ko01110
ZY_vs_ZM	Phenylpropanoid biosynthesis	144	1803	0	0	ko00940
	Biosynthesis of secondary metabolites	781	13,445	0	0	ko01110
	Plant hormone signal transduction	186	3317	2.87679E−10	3.8549E−08	ko04075
	Metabolic pathways	1225	26,138	1.04644E−39	1.40223E−37	ko01100
HY_vs_HM	Starch and sucrose metabolism	316	1896	0	0	ko00500
	Phenylpropanoid biosynthesis	692	1803	0	0	ko00940
	Biosynthesis of secondary metabolites	2564	13,445	0	0	ko01110
	Metabolic pathways	4141	26,138	2.7519E−186	3.8801E−184	ko01100

Note: Significant pathways were identified by corrected $P \leq 0.01$.

3.5. Differential anthocyanin transcription factor genes from three Chinese prickly ash cultivars

As far as structural genes are concerned, transcription factors also play an important role in regulating the overall activity of flavonoid biosynthesis. There were 119, 36, and 98 differentially expressed transcription factor genes analysed in CY_vs_CM, ZY_vs_ZM and HY_vs_HM, respectively, which were coded as MYB, bHLH, AP2/ERF, WRKY, HD-ZIP, HSF, NAC and Mads-box.

Almost all the different genes for MYB transcription factors were further attributed to the R2R3 MYB family, which is closely related to anthocyanin biosynthesis in fruit trees. There were 15, 11 and 15 differentially expressed MYB transcription factors in CY_vs_CM (Table S4, Fig. 3A), ZY_vs_ZM (Table S5, Fig. 3B), and HY_vs_HM (Table S6, Fig. 3C), respectively. Among the MYB DEGs, 12, 3 and 9 were upregulated in CY_vs_CM, ZY_vs_ZM, and HY_vs_HM, respectively. Four more highly expressed MYB genes in CM, but all with low FPKM values, and two MYB genes with low FPKM values were found in HM. The c80935, c226097 and c65290 genes were the transcription factors common to the three varieties, of which c80935 was upregulated, while c226097 was downregulated.

We further screened 10 MYB TFs, c8677, c209873, c80935, c226097, c65290, c50384, c57286, c104473, c91339, and c194504, which showed a high fold change in expression between the three cultivars and/or developmental stages. The MYB genes of c8677 in CM and c65290 in HM were significantly increased. Through protein sequence comparison (Fig. 3D), the gene c80935 was highly related to MdMYB10 of apple and plays a key role in the peel redness process. The gene c226097 was associated with the MYB transcription factor EsMYBA1 from *Epimedium sagittatum*, which can interact with several bHLH regulators of the flavonoid pathway and activate the promoters of DFR and ANS genes. The gene c65290 was highly similar to VvMYB5b of grape (*Vitis vinifera* L.), which leads to an upregulation of genes encoding enzymes of the flavonoid pathway and the accumulation of anthocyanin- and proanthocyanidin-derived compounds, whereas the gene c50384 was related to the anthocyanin activator groups, which was highly similar to VvMYBPA2 used for regulating anthocyanin biosynthesis in grapes. The gene c209873 was clustered with PpMYB9 of *Prunus persica*, which regulates the accumulation of anthocyanins in fruit peel. Fig. 3E shows the highly homologous R2 and R3 DNA-binding domains of R2R3-MYBs at the N-terminus (Espley et al., 2007) and a highly variable truncated C-terminal region, which might be related to Chinese prickly ash cultivar colour morph regulation.

The results showed that the activity of structural genes in the flavonoid biosynthesis pathway was regulated by other genes, such as MYB TFs. Our study was a good confirmation of these conclusions, as our transcription and metabolic group analyses highlight the main changes in MYB gene expression and interference with metabolites associated with flavonoid biosynthesis pathways, which might be the basis for changes in peel coloration. Therefore, we reconstructed flavonoid biosynthesis pathways and predicted the molecular mechanism of peel coloration. We found that most of the structural genes had high activity during the "green peel" but were downregulated during the mature period, while the ANS and UFGT genes had the opposite pattern. In general, MYB TFs had rigorous time-regulation of genes in the flavonoid biosynthesis pathway, which led to the accumulation of apigenin-7,4'-dimethylether, kaempferol-3,7-O-α-L-rhamnoside, apigenin5-O-glucoside, limocitrin 3,7-diglucoside, naringenin-7-O-triglycoside, pel-rha, pel-3,5-glu, peo-O-hex, cya-O-sya, and peo-3-O-glu at the mature stage, resulting in mature peels being red.

3.6. RT-qPCR validation of the transcriptomic data of Chinese prickly ash cultivars

To further verify the RNA-Seq results and the key genes involved in anthocyanin biosynthesis, we selected 12 genes, including the ANS genes (c158341, c97481), UFGT genes (c144425, c164027) and MYB regulatory genes (c80935, c226097), in the green peel and red peel of three Chinese prickly ash cultivars using RT-qPCR analysis. The expression patterns of these genes were very similar to the RNA-Seq results, which indicated that these genes may be associated with anthocyanin accumulation (Fig. 4.). The results showed the correlation between RNA-Seq data and RT-qPCR, which showed good consistency for both upregulated and downregulated gene expression.

4. Discussion

Similar to other fruits, the peel colour of Chinese prickly ash cultivars changes from green in the young fruit to red in the mature stage. To elucidate the molecular mechanism of colour change during the development process, our study selected three cultivars as experimental materials, used metabolomics and transcriptomics to determine the colour substance composition of the peel, identified the anthocyanins and flavonoids in the fruit peel, and analysed the key genes related to anthocyanin biosynthesis.

The metabolome analysis showed that a total of 43, 37, and 36 different metabolites were identified in Chinese prickly ash cultivars,

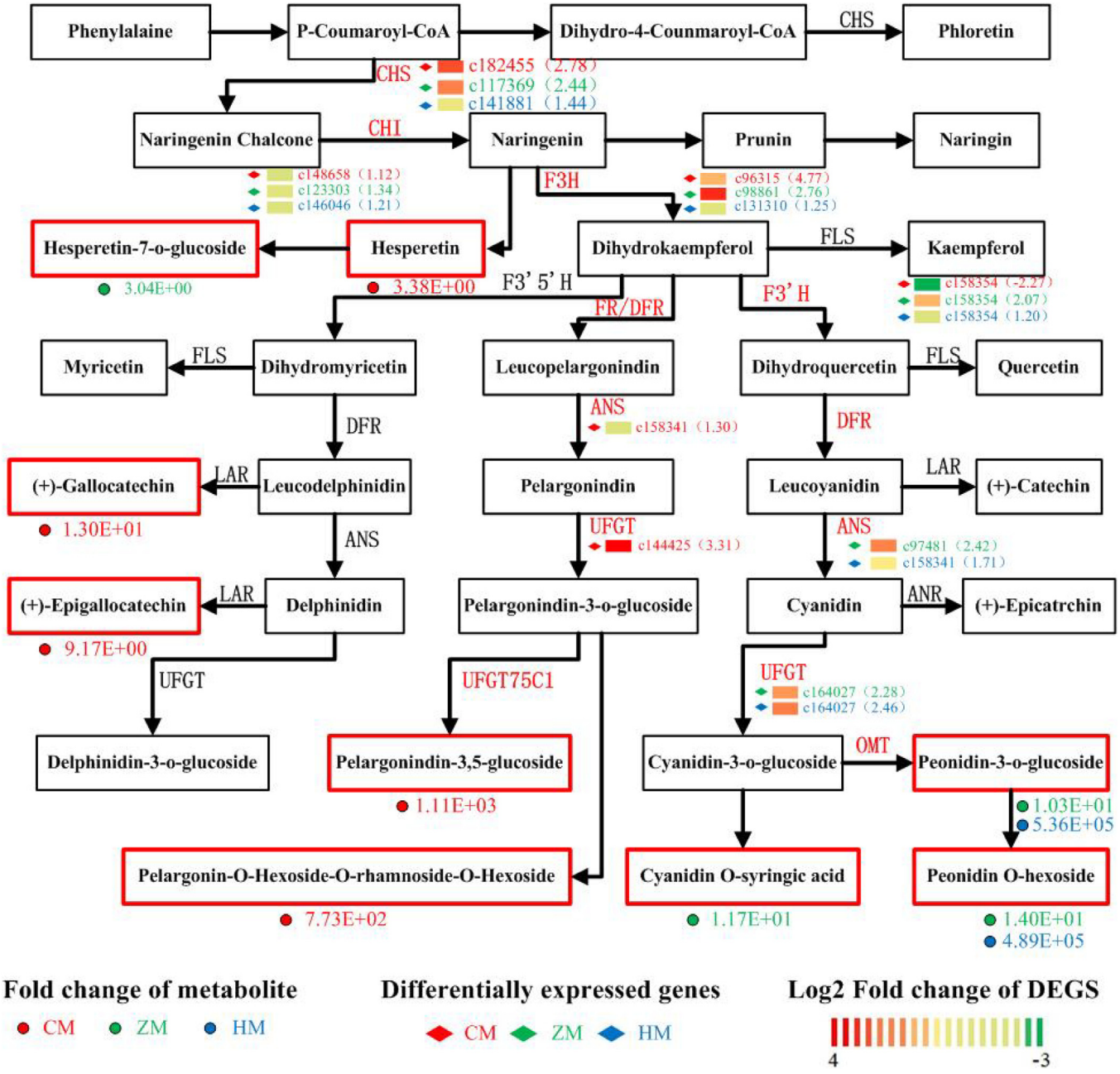

Fig. 2. Transcript profiling of genes in the phenylpropanoid and flavonoid biosynthetic pathways. Grids with colour-scale from green to red represent log2-fold change of DEGs. CHS, chalcone synthase; CHI, chalcone isomerase; F3H, flavanone 3-hydroxylase; F3′H, flavanoid 3′-hydroxylase; DFR, dihydroflavonol4-reductase; FR, flavanone 4-reductase; ANS, anthocyanidin synthase; UFGT, UDP glucose-flavonoid 3-O-glcosyl-transferase; FLS, flavonol synthesis; LAR, leucocyanidin reductase; ANR, anthocyanin reductase. (For interpretation of the references to colour in this figure legend, the reader is referred to the web version of this article.)

including 5, 6, and 4 species of anthocyanins and 38, 31, and 32 kinds of flavonoid contents. Through the different metabolites accumulated during the mature process, it was found that flavonoids were the main metabolites that regulated the redness of Chinese prickly ash fruits. Flavonoids are the main molecules involved in plant pigmentation (Zhou et al., 2020). Anthocyanins are the most important flavonoid pigments in plants (Baldi et al., 2018; Hong et al., 2020). No studies have been conducted to investigate the role of anthocyanins in Chinese prickly ash peel coloration. However, in our study, we found that pel-rha, pel-3,5-diglu, peo-O-hex, cya-O-sya, and peo-3-O-glu were the key anthocyanins in peels at the mature periods. Meanwhile, pel-rha and pel-3,5-diglu are reported to give a red coloration in plant *Chilean pomegranate* (Sepulveda et al., 2010); peo-O-hex and cya-O-sya were identified in the red colour of *Michelia maudiae* rubellis tepals (Lang et al., 2019).

In general, two types of genes in plants are involved in anthocyanin biosynthesis: the first type is the structural genes that encode enzymes to catalyse anthocyanin biosynthesis (Liu et al., 2020; Ma et al., 2018) and the second type is the regulatory genes that control the transcription of these structural genes (Kondo et al., 2002; Wang et al., 2013). Through KEGG enrichment and gene function annotation analysis, the DEGs related to flavonoid synthesis (PAL, C4H, 4CL, CHS, CHI, F3′H, FLS, ANS, UFGT, LAR and ANR) were identified from three varieties, of which most structural genes in the anthocyanin biosynthesis

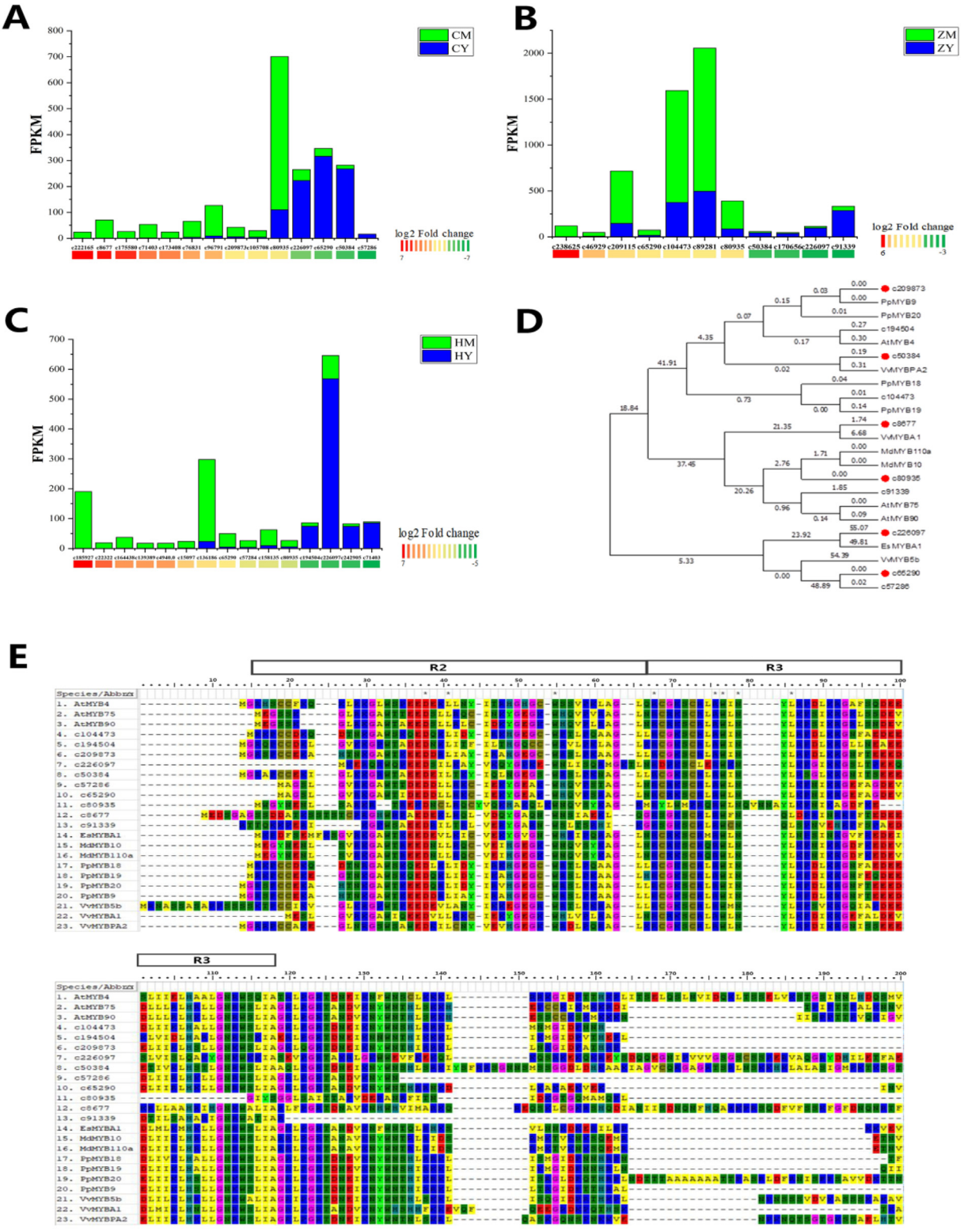

Fig. 3. Differentially expressed MYB genes between "CY_vs_CM", "ZY_vs_ZM" and "HY_vs_HM". (A) Differentially expressed MYB genes between "CY_vs_CM". (B) Differentially expressed MYB genes between "ZY_vs_ZM". (C) Differentially expressed MYB genes between "HY_vs_HM". (D) Phylogenetic analysis of 10 MYB genes. (E) R_2R_3-MYB protein sequence alignment of 10 MYB genes recruited by high fold expression change; R_2R_3 motif is indicated at the top.

pathway were upregulated. The ANS and UFGT genes involved in the final steps of the flavonoid biosynthetic pathway (biosynthesis and accumulation of anthocyanins) were gradually activated during maturation. Anthocyanidins are highly unstable and easily susceptible to degradation; therefore, glycosylation is essential to stabilize them and serve as a signal for the transport of anthocyanins to vacuoles, where they can function as pigments. This role is played by UFGT genes. Our study suggested that three ANS genes (c158341, c15481,

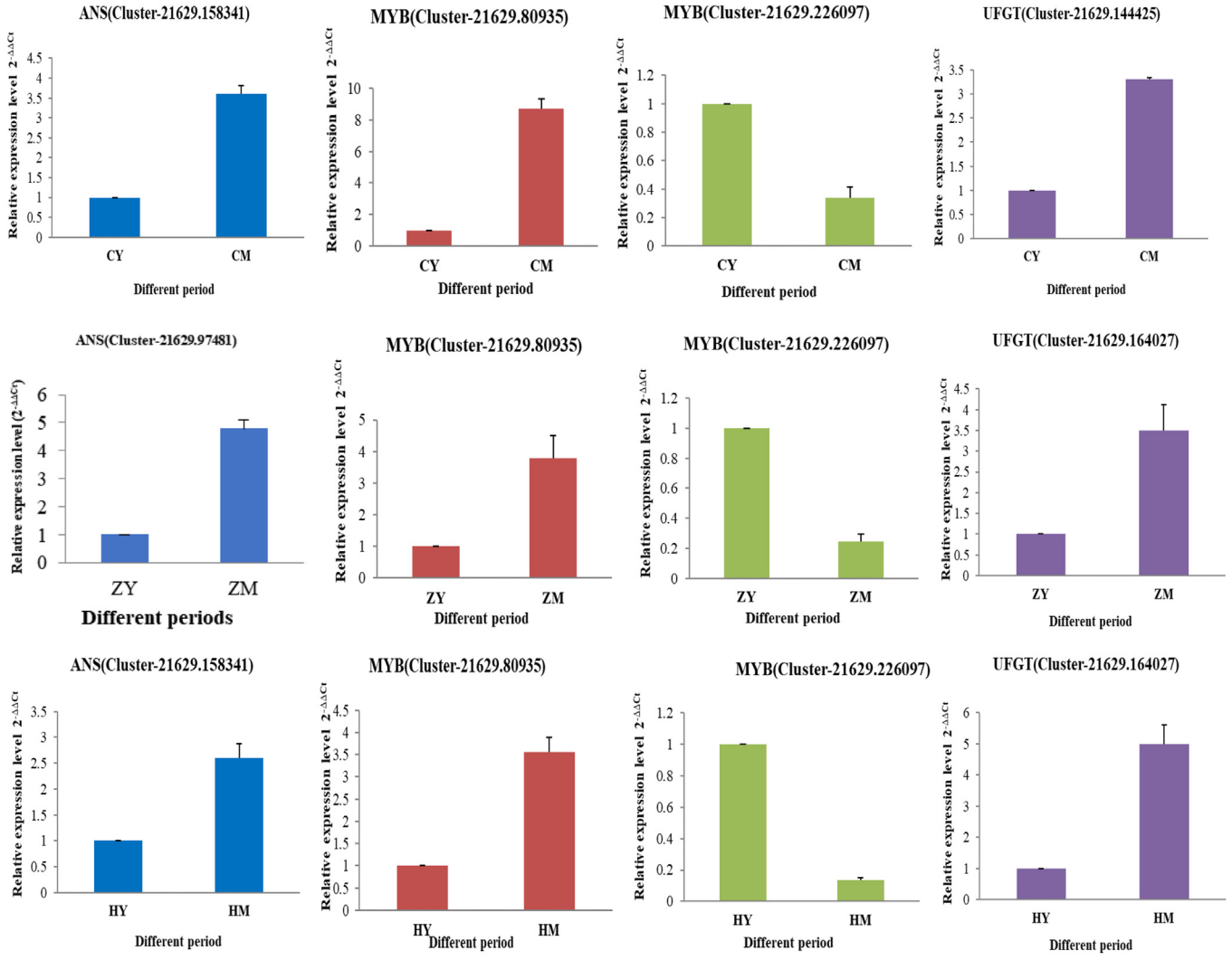

Fig. 4. Expression analysis of anthocyanin biosynthetic genes at different periods in green and red peels from three *Zanthoxylum* L. cultivars. (For interpretation of the references to colour in this figure legend, the reader is referred to the web version of this article.)

c97481) and three UFGT genes (c144425, c164027, c164027) were consistent with the amounts of anthocyanins in the peels, suggesting that these genes may be the key genes for anthocyanin biosynthesis. The pigment content and expression level of the ANS genes were both significantly higher in red radish (*Raphanus sativus* L.), and the UFGT genes of grape were reported to regulate anthocyanin biosynthesis during reddening (Jeong et al., 2004).

Anthocyanin biosynthesis is mainly regulated by transcription factors, and MYB transcription factors are the key transcription factors of the anthocyanin biosynthesis pathway genes of fruits, which activate the activity of the upstream promoter of the structural gene (Tai et al., 2014; Tang et al., 2020). The MdMYB10 and MdMYB110a genes in *Malus* × *domestica*, cloned from red pulp apples 'Red Field' and 'Sangrado', respectively, have been shown to positively regulate type I/II apple peel colour (Hamada et al., 2015) and are responsible for controlling anthocyanin biosynthesis in apple fruit (Espley et al., 2007). The EsMYBA1 transcription factors in *Epimedium sagittatum* were shown to regulate the biosynthesis of anthocyanin and flavonoid active ingredients (Huang et al., 2015). In addition, the VvMYB5b transcription factor in grapes is the initiator of genes involved in anthocyanin and procyanidin biosynthesis, which positively regulates the biosynthesis of tannic acid and anthocyanins while inhibiting lignin metabolism pathways (Huang et al., 2013), and VvMYBF1 actively regulates flavonoid biosynthesis in grapes by controlling the gene expression of flavonoid synostic synthase-1 (VvFLS1) (Czemmel et al., 2009). In jujube peel and *Camellia sinensis*, the MYB genes and HD-Zip TFs may have similar functions in flavonoid biosynthesis (Zhang et al., 2020, 2019). We also found that the expression patterns of c80935 and c226097 in differential transcription factors were similar to the structural genes ANS and UFGT, and the expression trends of those transcription factors were closely related to the content of pel-rha, pel-3,5-diglu, peo-O-hex, cya-O-sya, and peo-3-O-glu. Therefore, these results suggested that the c80935 and c226097 genes may be the key regulatory factors for anthocyanin biosynthesis in three Chinese prickly ash cultivars.

5. Conclusion

In summary, the anthocyanin accumulation mechanisms of Chinese prickly ash peels at the mature stage were studied using metabolomics and transcriptomics technology. There was a significant difference in the variation of flavonoid metabolites, particularly the high accumulation of pel-rha, pel-3,5-diglu, peo-O-hex, cya-O-sya, and peo-3-O-glu, which explained the redness of the mature peels. Moreover, we determined and identified differentially expressed structural genes and transcription factors involved in anthocyanin biosynthesis and found

gene regulatory patterns of the flavonoid biosynthesis pathway. Through the correlation analysis of metabolome and transcriptome approaches, the key genes of anthocyanin biosynthesis and the molecular mechanism of anthocyanin biosynthesis were further understood. Our results also provided new insight into anthocyanin accumulation and the molecular mechanism and identified a series of candidate genes to cultivate anthocyanin-rich varieties.

Author contributions

Tao Zheng and Shu-Ming Liu conceived and designed the experiments, Tao Zheng analysed the data, Ke-xing Su modified the picture, Tao Zheng wrote the paper, and all authors have read and approved the manuscript for publication.

Declaration of Competing Interest

The authors declare that they have no known competing financial interests or personal relationships that could have appeared to influence the work reported in this paper.

Acknowledgements

This article was supported by the project “The demonstration and promotion of efficient cultivation and management techniques of Zanthoxylum bungeanum in Hanyuan Weibei”.

Appendix A. Supplementary data

Supplementary data to this article can be found online at https://doi.org/10.1016/j.fochms.2020.100004.

References

Artaria, C. et al (2011). Lifting properties of the alkamide fraction from the fruit husks of zanthoxylum bungeanum.*Int. Journal of Cosmetic Science, 33*, 328–333.
Baldi, P. et al (2018). Gene expression and metabolite accumulation during strawberry (fragaria x ananassa) fruit development and ripening. *Planta, 248*, 1143–1157.
Chen, W. F., et al. (2019). Differential regulation of anthocyanin synthesis in apple peel under different sunlight intensities. International Journal of Molecular Sciences,20,
Chen, X. et al (2019). Quality evaluation and chemometric discrimination of zanthoxylum bungeanum maxim leaves based on flavonoids profiles, bioactivity and hplc-fingerprint in a common garden experiment. *Industrial Crops and Products, 134*, 225–233.
Cho, K. et al (2016). Network analysis of the metabolome and transcriptome reveals novel regulation of potato pigmentation. *Journal of Experimental Botany, 67*, 1519–1533.
Czemmel, S. et al (2009). The grapevine r2r3-myb transcription factor vvmybf1 regulates flavonol synthesis in developing grape berries. *Plant Physiology, 151*, 1513–1530.
Dong, T. T. et al (2019). Anthocyanins accumulation and molecular analysis of correlated genes by metabolome and transcriptome in green and purple asparaguses (asparagus officinalis, l.). *Food Chemistry, 271*, 18–28.
Ellinger, S. et al (2012). Bolus consumption of a specifically designed fruit juice rich in anthocyanins and ascorbic acid did not influence markers of antioxidative defense in healthy humans. *Journal of Agricultural and Food Chemistry, 60*, 11292–11300.
Espley, R. V. et al (2007). Red colouration in apple fruit is due to the activity of the myb transcription factor, mdmyb10. *Plant Journal, 49*, 414–427.
Fragoso, M. F. et al (2018). Lyophilized acai pulp (euterpe oleracea mart) attenuates colitis-associated colon carcinogenesis while its main anthocyanin has the potential to affect the motility of colon cancer cells. *Food and Chemical Toxicology, 121*, 237–245.
Gao, H. Y. et al (2020). Transcriptomics and metabolomics analyses reveal the differential accumulation of phenylpropanoids between cinnamomum cassia presl and cinnamomum cassia presl var. Macrophyllum chu. *Industrial Crops and Products, 148*.
Gharibi, S. et al (2019). The effect of drought stress on polyphenolic compounds and expression of flavonoid biosynthesis related genes in achillea pachycephala rech. F.. *Phytochemistry, 162*, 90–98.
Hamada, Y. et al (2015). Breeding depression of red flesh apple progeny containing both functional mdmyb10 and myb110a_jp genes. *Plant Breeding, 134*, 239–246.
Hodaei, M. et al (2018). The effect of water stress on phytochemical accumulation, bioactive compounds and expression of key genes involved in flavonoid biosynthesis in chrysanthemum morifolium l. *Industrial Crops and Products, 120*, 295–304.
Hong, H. T., et al. (2020). Optimisation of extraction procedure and development of lc-dad-ms methodology for anthocyanin analysis in anthocyanin-pigmented corn kernels. Food Chemistry,319,
Huang, W. J., et al. (2013). A r2r3-myb transcription factor from epimedium sagittatum regulates the flavonoid biosynthetic pathway. Plos One, 8,
Jaakola, L. (2013). New insights into the regulation of anthocyanin biosynthesis in fruits. *Trends in Plant Science, 18*, 477–483.
Jeong, S. T. et al (2004). Effects of plant hormones and shading on the accumulation of anthocyanins and the expression of anthocyanin biosynthetic genes in grape berry skins. *Plant Science, 167*, 247–252.
Jin, J., et al. (2019). Differential gene expression and associated metabolite accumulation in fungus ophiocordyceps xuefengensis cultivated under breathable and airtight conditions.Mycoscience,60, 281-286.
Kondo, S. et al (2002). Changes in the expression of anthocyanin biosynthetic genes during apple development. *Journal of the American Society for Horticultural Science, 127*, 971–976.
Kruger, M. J. et al (2014). Proanthocyanidins, anthocyanins and cardiovascular diseases. *Food Research International, 59*, 41–52.
Lang, X. A., et al. (2019). Integrated metabolome and transcriptome analysis uncovers the role of anthocyanin metabolism in michelia maudiae. International Journal of Genomics, 2019.
Li, D. et al (2020). Metabolic profiling and transcriptome analysis of mulberry leaves provide insights into flavonoid biosynthesis. *Journal of Agricultural and Food Chemistry, 68*, 1494–1504.
Li, P. M. et al (2013). Primary and secondary metabolism in the sun-exposed peel and the shaded peel of apple fruit. *Physiologia Plantarum, 148*, 9–24.
Liao, Y., et al. (2014). Featurecounts: An efficient general purpose program for assigning sequence reads to genomic features.Bioinformatics, 30, 923-930.
Liu, C. Q., et al. (2020). Transcriptomic profiling of purple broccoli reveals light-induced anthocyanin biosynthetic signaling and structural genes. PeerJ, 8.
Liu, M. Y. et al (2016). The effects of light and ethylene and their interaction on the regulation of proanthocyanidin and anthocyanin synthesis in the skins of vitis vinifera berries. *Plant Growth Regulation, 79*, 377–390.
Liu, X. Y. et al (2019). effect and mechanism of essential oil from zanthoxylum bungeanum in microemulsion gel preparation on percutaneous delivery of complex components. *Zhongguo Zhong Yao Za Zhi, 44*, 4627–4633.
Liu, Y. et al (2018). Anthocyanin biosynthesis and degradation mechanisms in solanaceous vegetables: A review. *Frontiers in Chemistry, 6*.
Lu, L. H. et al (2020). Metabolomics analysis reveals perturbations of cerebrocortical metabolic pathways in the pah(enu2) mouse model of phenylketonuria. *CNS Neuroscience & Therapeutics, 26*, 486–493.
Ma, Y. J., et al. (2018). Transcriptomic analysis of lycium ruthenicum murr. During fruit ripening provides insight into structural and regulatory genes in the anthocyanin biosynthetic pathway. Plos One, 13.
Milbury, P. (2015). Anthocyanin metabolism and transport across the blood brain barrier. Abstracts of Papers of the American Chemical Society, 250,
Ohno, S. et al (2011). A bhlh transcription factor, dvivs, is involved in regulation of anthocyanin synthesis in dahlia (dahlia variabilis). *Journal of Experimental Botany, 62*, 5105–5116.
Petroni, K., & Tonelli, C. (2011). Recent advances on the regulation of anthocyanin synthesis in reproductive organs. *Plant Science, 181*, 219–229.
Pojer, E. et al (2013). The case for anthocyanin consumption to promote human health: A review. *Comprehensive Reviews in Food Science and Food Safety, 12*, 483–508.
Polturak, G. et al (2018). Transcriptome and metabolic profiling provides insights into betalain biosynthesis and evolution in mirabilis jalapa. *Molecular Plant, 11*, 189–204.
Poulose, S. M. et al (2012). Anthocyanin-rich acai (euterpe oleracea mart.) fruit pulp fractions attenuate inflammatory stress signaling in mouse brain bv-2 microglial cells. *Journal of Agricultural and Food Chemistry, 60*, 1084–1093.
Rothenberg, D. O., et al. (2019). Metabolome and transcriptome sequencing analysis reveals anthocyanin metabolism in pink flowers of anthocyanin-rich tea (camellia sinensis). Molecules, 24.
Saito, K. et al (2013). The flavonoid biosynthetic pathway in arabidopsis: Structural and genetic diversity. *Plant Physiology and Biochemistry, 72*, 21–34.
Sepulveda, E. et al (2010). Influence of the genotype on the anthocyanin composition, antioxidant capacity and color of chilean pomegranate (punica granatum l.) juices. *Chilean Journal of Agricultural Research, 70*, 50–57.
Shoeva, O. Y. et al (2014). The regulation of anthocyanin synthesis in the wheat pericarp. *Molecules, 19*, 20266–20279.
Sun, L. et al (2019). Comparative transcriptome analysis and expression of genes reveal the biosynthesis and accumulation patterns of key flavonoids in different varieties of zanthoxylum bungeanum leaves. *Journal of Agricultural and Food Chemistry, 67*, 13258–13268.
Tai, D. Q., et al. (2014). A malus crabapple chalcone synthase gene, mcchs, regulates red petal colour and flavonoid biosynthesis. Plos One, 9,
Tang, R. F., et al. (2020). Involvement of mirna-mediated anthocyanin and energy metabolism in the storability of litchi fruit. Postharvest Biology and Technology, 165.
Wang, L. X. et al (2013). The effect of fruit bagging on the color, phenolic compounds and expression of the anthocyanin biosynthetic and regulatory genes on the 'granny smith' apples. *European Food Research and Technology, 237*, 875–885.
Wang, Z. et al (2017). Regulation of fig (ficus carica l.) fruit color: Metabolomic and transcriptomic analyses of the flavonoid biosynthetic pathway. *Frontiers in Plant Science, 8*, 1990.
Wang, Z. G. et al (2017). Transcriptome analysis reveals candidate genes related to color fading of 'red bartlett' (pyrus communis l.). *Frontiers in Plant Science, 8*.
Winkel-Shirley, B. (2002). Biosynthesis of flavonoids and effects of stress. *Current Opinion in Plant Biology, 5*, 218–223.

Wu, Z. et al (2018). Simultaneous enrichment and separation of four flavonoids from zanthoxylum bungeanum leaves by ultrasound-assisted extraction and macroporous resins with evaluation of antioxidant activities. *Journal of Food Science, 83*, 2109–2118.

Yang, F. X. et al (2008). Studies on the preparation of biodiesel from zanthoxylum bungeanum maxim seed oil. *Journal of Agricultural and Food Chemistry, 56*, 7891–7896.

Yu, L. et al (2020). Quality evaluation of different varieties of zanthoxylum bungeanum maxim. Peels based on phenolic profiles, bioactivity, and hplc fingerprint. *Journal of Food Science, 85*, 1090–1097.

Zhang, L. H. et al (2016). Tea polyphenols incorporated into alginate-based edible coating for quality maintenance of Chinese winter jujube under ambient temperature. *Lwt-Food Science and Technology, 70*, 155–161.

Zhang, Q. et al (2020). Transcriptome and metabolome profiling unveil the mechanisms of ziziphus jujuba mill. Peel coloration. *Food Chemistry, 312*.

Zhang, Q. F., et al. (2017). Metabolomics analysis reveals the metabolic and functional roles of flavonoids in light-sensitive tea leaves. BMC Plant Biology, 17.

Zhang, X. Y. et al (2019). Athb2, a class ii hd-zip protein, negatively regulates the expression of csans, which encodes a key enzyme in camellia sinensis catechin biosynthesis. *Physiologia Plantarum, 166*, 936–945.

Zhang, Y. J. et al (2015). Anthocyanin accumulation and molecular analysis of correlated genes in purple kohlrabi (brassica oleracea var. Gongylodes l.). *Journal of Agricultural and Food Chemistry, 63*, 4160–4169.

Zhou, H. et al (2015). Molecular genetics of blood-fleshed peach reveals activation of anthocyanin biosynthesis by nac transcription factors. *Plant Journal, 82*, 105–121.

Zhou, X. J., et al. (2020). A novel microfluidic aqueous two-phase system with immobilized enzyme enhances cyanidin-3-o-glucoside content in red pigments from mulberry fruits.Biochemical Engineering Journal, 158,

Zhuang, H., et al. (2019). Differential regulation of anthocyanins in green and purple turnips revealed by combined de novo transcriptome and metabolome analysis. International Journal of Molecular Sciences, 20.